Harmonic resonance risk of massive ultra fast charging station grid integration

DOI:
10.1109/ICHQP.2018.8378897

Document status and date:
Published: 08/06/2018

Document Version:
Publisher’s PDF, also known as Version of Record (includes final page, issue and volume numbers)

Harmonic Resonance Risk of Massive Ultra Fast Charging Station Grid Integration

Y. Sun, E. C. W. de Jong
Electrical Energy System
Technical University Eindhoven
Eindhoven, the Netherlands
Email: y.sun@tue.nl

V. Cuk and J. F. G. Cobben
Electrical Energy System
Eindhoven, the Netherlands
Technical University Eindhoven
Email: v.cuk@tue.nl

***Abstract*—Plug-in electric vehicle (PEV) is gaining steadily preference among consumers as they offer economically viable and environmentally friendly transportation solutions when compared to their gasoline powered counterparts. A decent charging station network coverage has been identified as the main enabler for the adoption of PEV. Therefore, the availability of ultra-fast charging station (UFCS) is not only a technical prerequisite but also a key enabler for the consumer acceptance to bring the electric mobility to the next level. To facilitate the smooth integration of UFCS in the existing power grid, hence rapid uptake rate of PEV, this article elaborates on the analytical derivation of the norton equivalent for the study of harmonic resonance when several UFCSs are connected to the local medium voltage (MV) grid. The impedance of norton equivalent model explicitly represents the input admittance of power converter under small signal perturbation. A case study is performed on the Dutch Bronsbergen MV grid to which 10 UFCSs are connected and its impact on the grid resonance point is shown with harmonic distortion calculation.**

I. Introduction

PEV is gaining steadily preference among consumers as they offer economically viable and environmentally friendly transportation solutions when compared to their gasoline powered counterparts. Despite improved travel range offered by popular PEV models (e.g. Tesla Model S, Nissan Leaf, General Motor Bolt etc.) the battery charging facility nowadays does not offer the same level of convenience for the PEV owners as oppose to the extensive gasoline station network. Even though the level 1 household plug can easily refill the battery over the night, it does not offer the PEV owner the freedom for long distance travel and "range anxiety" free feeling. The Tokyo electric power company (TEPCO) study published in 2008 and BMW research project "Mini E" conducted in the cities of Los Angeles, Berlin, and London [1] both confirm that the public charging infrastructure such as the ultra-fast charging station (UFCS) plays a key role in the development of the electromobility and transition towards E-mobility travel routine. In a report [2] revealing the historical lessons learnt from Norwegian experience in the deployment of electric vehicle, a decent charging station network coverage has been identified as the main enabler for the adoption of PEV. Therefore, the availability of UFCS is not only a technical prerequisite but also a key enabler for the consumer acceptance to bring the electric mobility to the next level. Recognizing the need for UFCS, numerous literatures investigated the methodology to find the optimal UFCS locations taking into account the spatial and temporal transportation behaviour [3], the service range in combination with the power network constraint [4][5], and the installation cost in specific cases such as Barcelona [6] and Iran [7]. While the optimal location of UFCS present only one side of the equation, the successful deployment of UFCS highly depends on the existing grid hosting capability since the UFCS provides level 3 off-board DC charging slot (output power range from 90kW to 240kW) as specified by the Association of Automotive Engineers (SAE) imposing potential risk of congestion and violation of voltage in the local medium voltage (MV) grid. Stochastic load flow is the typical approach to identify the potential grid voltage profile violation and component overloading in the UFCS integration study as elaborated in [8][9][10][11][12]. Two case study on the Italian MV distribution network is presented in [13][14] suggesting viable mitigation measures such as an UFCS with stationary battery storage. Next to the static analysis for the integration of UFCS, the transient dynamic analysis of UFCS grid integration is also studied in the [15][16]. Despite a paper found on the power quality issues of UFCS, it is only limited to the typical North American residential building level power quality improvement using the UFCS as an innovative multilevel transformerless Hybrid Series Active Filter[17]. To the best knowledge of the author, the impact of UFCS on the MV grid harmonic resonance is not addressed in previous literatures, hence deserve a detailed investigation. A UFCS offering several level 3 charging slots connecting to the MV grid could easily reach MW (250kW x 4) level, its harmonic emission to the MV grid should be assessed. The widespread deployment of UFCSs with an active front end (AFE) can also adversely impact the local MV grid impedance resonance point causing hazardous harmonic resonances threat to the distribution network operators (DNOs). This article focuses on the proper modelling of UFCS with an AFE in the harmonic resonance study and provide additional system impact analysis via a study case of MV grid in Bronsbergen, the Netherlands.

978-1-5386-0517-2/18/ $31.00 ©2018 IEEE

II. UFCS Topology and Model

A vast amount of Innovative UFCS converter topologies exists in the literatures as well as the manufacture product offers [18]. When the AFE is directly coupled to the MV grid, three level neutral point clamp [19], cascaded H-bridge [20], matrix [21] inverter topologies are found in the literatures for the active front end realization whilst galvanic isolation is provided by a dual active bridge DC/DC stage interfaced to the PEV battery. When the galvanic isolation is provided by the low frequency MV/LV power transformer, 2-level AFE and its variation are common design approach reported in literatures [22][23]. To ease the impact of UFCS surge current on the power grid, stationary battery storage provides the necessary buffer [24][25][18] with possible application specific bundling options such as: superconducting magnetic energy storage [26], flywheel [27], and supercapacitor bank [28]. For this study, it is not possible to capture all the aforementioned UFCS topologies reported in the literatures. To illustrate the impact of a typical future UFCS on the power grid resonance behaviour, a simple 2-level AFE with stationary battery storage topology is chosen for this study due to its prevailing presence in the literature and technology readiness for the mass production. Fig. 1 demonstrates the generic UFCS topology for this study, where the active front end (1MW) is coupled to the medium voltage grid via a 10/0.4 kV transformer while each level 3 charging slot (250 kW x 4) is connected to the UFCS DC link via a DC/DC converter. The stationary battery storage device is then connected to the UFCS DC link via a dedicated DC/DC converter to reduce the static impact (power grid congestion, component overloading etc.) of UFCS on the local medium voltage grid. Once the generic UFCS topology is

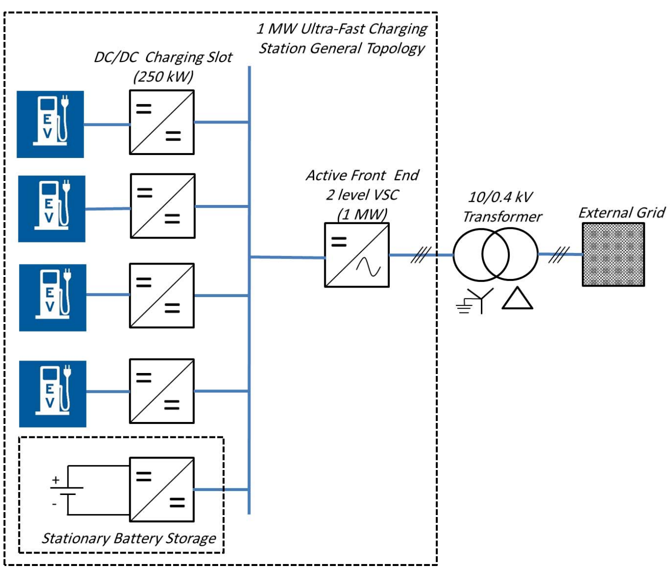

Fig. 1. Typical UFCS topology with 2-level active front end and stationary battery storage

determined, an electromagnetic transient (EMT) model of the UFCS can be built in EMTDC/PSCAD V4.6.2 to study its impact on the MV grid to which it connects. Since the UFCS transient dynamic electrical characteristic seen from the power grid is mainly dictated by the AFE, for the EMT model the DC side charging slot and stationary battery storage DC/DC circuit is simplified to an ideal DC current source connected to the DC link of AFE grid side inverter as shown in Fig.2. For this paper, the EMTDC/PSCAD model built for UFCS is only to confirm the AFE controller parameters, based on which the input admittance of AFE is analytically derived in section III-B. The main control and electrical parameter

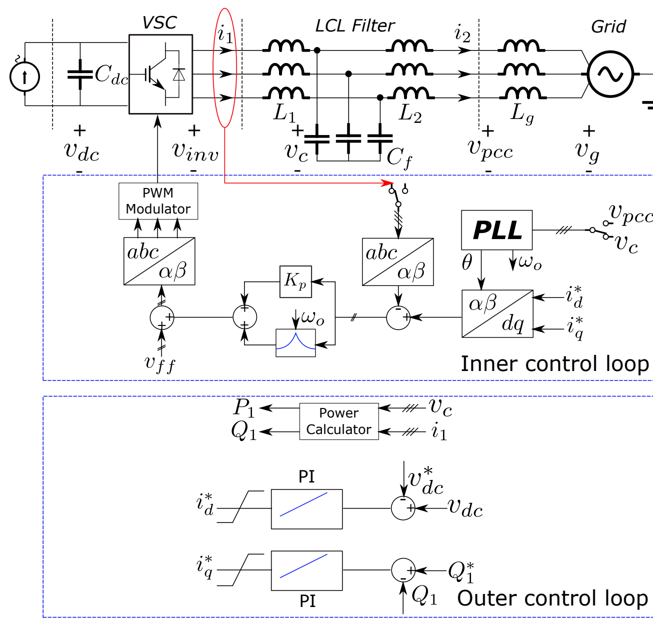

Fig. 2. UFCS 2 level active front end with simplified DC circuit

chosen for the 1MW UFCS is shown in the Table. I. A typical cascaded control scheme is assigned to the 1MW UFCS simulation model as shown in Fig. 2, where the outer-loops are realized by two parallel proportional integral (PI) controllers regulating the DC bus voltage and the reactive power output to constant respectively and the inner-loop is realized by proportional resonance controllers regulating the AFE grid side current dynamics. Reference value is indicated with $*$ in their superscript. In Fig.2, v_{ff} is the feed-forward voltage in $\alpha\beta$ frame, v_c is the filter capacitor instantaneous phase to neutral voltage in abc frame, i_1 is the inverter side instantaneous current in abc frame, i_d^* and i_q^* are the current control loop references in-phase and quadrature with the grid voltage (i.e. v_c) in dq frame, P_1 and Q_1 are active and reactive power calculated at the filter capacitor side, v_{dc} and v_{dc}^* are DC voltage and its reference set-point respectively.

III. VSC Model for Harmonic Analysis

This section starts with a short introduction on the evolution of the power system harmonic distortion calculation and the associated harmonic source model, followed by a discussion

TABLE I
VSC CONVERTER DESIGN PARAMETERS

Parameter	Value	Unit
S_r Rated Power	1000	kW
V_{dc} DC Link Voltage	800	Volts
C_{dc} DC Link Capacitor	20	mF
V_{rms} AC voltage	400	Volts
L_1 Inverter Side Inductor	100	μH
R_1 Resistance of L_1	0.001	Ohm
L_2 Grid Side Inductor	48.5	μH
R_2 Resistance of L_2	0.001	Ohm
C_f Filter Capacitor	400	μF
R_f ESR of C_f	0.01	Ohm
T_s Sampling Time	100	μs
f_{sw} Switching Frequency	5000	Hertz
K_p PR Proportional Gain	1	p.u.
K_i PR Integral Gain	250	p.u.
ω_c PR Bandwidth	2	p.u.
$K_{pv_{dc}}$ DC Proportional Gain	1	p.u.
$K_{iv_{dc}}$ DC Integral Gain	100	p.u.
K_{p_Q} Q Proportional Gain	1	p.u.
K_{i_Q} Q Integral Gain	100	p.u.

of the issues related to the ideal current source model. Then the state-of-the-art modelling approach (i.e converter harmonic model) in representing the input admittance of VSC is given.

A. Background on the harmonic modelling development

The typical method used for the modelling of harmonic-generating devices is the ideal (constant) current source model. This approach originated from times when the line commutated harmonic-generating devices (i.e. load-commutated converters and diode rectifiers) dominated. It has since been proven to be inaccurate for the modelling of self-commutated devices (e.g. VSC high voltage direct current station, doubly-fed induction generator, photovoltaic, full converter based wind turbine, UFCS). Even though it is common practice to measure harmonic current emission at the grid connection point, such harmonic current emission measurements should not be used for the representation of VSC based power electronics as an equivalent ideal current source in the harmonic resonance analysis [29], as will be substantiated next. The reasons are three folds: firstly, the measurement is not performed in a clean grid environment, i.e. without background harmonic distortion. Secondly, an ideal current source fails to capture the converter control reaction to the background harmonic voltage. Lastly for the network impedance scan, an ideal current source does not present the frequency dependent inner current control loop and the passive output filter resulting in an inaccurate network resonance point estimation.

B. Derivation of VSC input-admittance

Frequency domain approach is proposed by the researchers to represent VSC devices with its input admittance characteristics seen from the AC grid. Early papers published on the frequency domain input admittance representation of VSC device has proven to be effective, as the theoretical calculation demonstrate close agreement with the kW range laboratory setup validation results. [30] presents the input admittance derivation of a single phase inverter using only PI control for the inner current control loop, while [31] advances analysis to consider a typical three phase grid-connected VSC with the typical dq synchronous frame control strategy for its inner current control loop. [32] and [33] further elaborates on the influence of PLL in the determination of VSC input admittance characteristic. For the analysis of UFCS, when its PLL is designed with typical low bandwidth, the non-linear effect of PLL on the grid side VSC input admittance characteristics can be omitted without causing significant errors [33]. Therefore in this paper, we calculates the VSC input admittance characteristics via analytical transfer function derivation without considering the PLL effect. For the VSC converter, its inner current loop transfer function with PLL impact can be represented as Fig. 3 [33]:

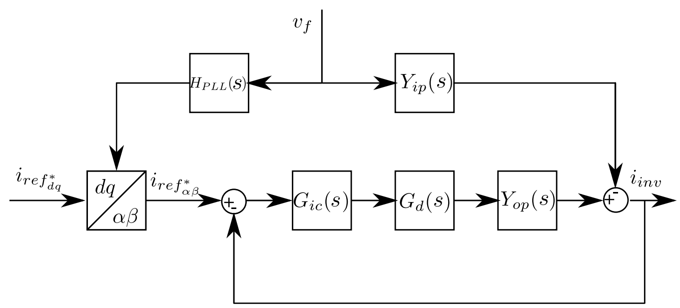

Fig. 3. VSC close loop continuous transfer function diagram

C. Converter Impedance Model without PLL Effect

The transfer function without considering the PLL impact can be first shown as in Fig.4:

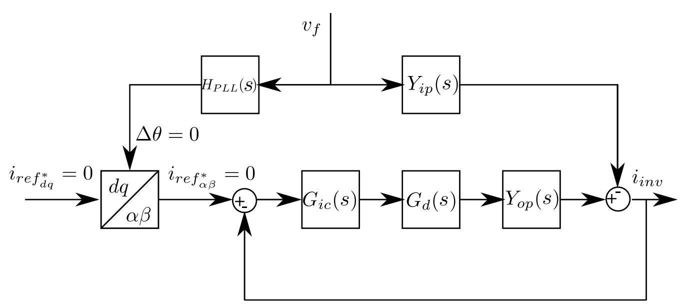

Fig. 4. VSC close loop continuous transfer function diagram without PLL impact

For its close loop transfer function, the following equations can be written:

$$-v_f Y_{ip}(s) - i_{inv} G_{ic}(s) G_d(s) Y_{op}(s) = i_{inv} \tag{1}$$

$$-i_{inv} - i_{inv} G_{ic}(s) G_d(s) Y_{op} = v_f Y_{ip}(s) \tag{2}$$

The input admittance of VSC can be determined by solving (1) and (2) for the $G_{tcl}(s) = \frac{v_f}{-i_{inv}}$ when the current control reference is maintained the same (i.e. $i_{ref^*_{dq}} = 0$) and PLL effect is not considered (i.e. $\Delta\theta = 0$):

$$G_{tcl}(s) = \frac{v_f}{-i_{inv}}\Big|_{\Delta\theta=0, i_{ref^*_{dq}}=0} = \frac{G_{ic}(s) G_d(s) Y_{op}(s) + 1}{Y_{ip}(s)} \tag{3}$$

$G_{ic}(s)$ depicts the proportional resonance controller in s domain :

$$G_{ic}(s) = K_p + \frac{2K_i\omega_c}{s^2 + 2\omega_c s + \omega_o^2} \tag{4}$$

$G_d(s)$ indicates one an half sampling cycle delay caused by the digital computation and the PWM zero-order hold effect respectively [34]:

$$G_d(s) = e^{-1.5T_s s} \tag{5}$$

$Y_{ip}(s)$ and $Y_{op}(s)$ are the admittance of inverter side inductor:

$$Y_{ip}(s) = Y_{op}(s) = \frac{1}{L_1 s + R_1} \tag{6}$$

Applying the parameters from Table I, then the VSC input admittance $G_{tcl}(s)$ shown as norton equivalent (red in Fig. 5(a)) can be plotted in bode diagram (Fig. 5(b)), where inverter side inductor plus the VSC control is shown in blue and inverter side passive inductor frequency characteristic alone is shown in orange. The harmonic current emission from UFCS on the inverter side of inductor is taken from PSCAD simulation and shown in Fig. 5(c), where switching harmonics sdie bands are clearly visible at the integer times of PWM switching frequency (i.e. 5kHz = 100^{th} harmonic order)

IV. Harmonic Resonance Analysis in Dutch MV Grid

A typical Dutch MV grid in Bronsbergen (Fig. 6) operated by Alliander (Dutch DNO) has been selected for the case study to reveal the potential harmonic resonance risk in the case of massive UFCS grid integration. The UFCSs are connected at the MV bus 12 (Roelofs), where its downstream LV grid is represented in detail.

The impedance sweep is calculated at MV bus 12 (Roelofs) for two scenarios: base case without UFCS connection, 10 UFCS connections with the converter harmonic model. Fig. 7 presents the results of the impedance sweep (blue-base case without the UFCS connection, red-10 UFCS connections with the converter harmonic model). It is clear from the impedance sweep results that the original network resonance point (i.e 1600 Hz) will shift towards 1250 Hz as a result of the UFCS connections despite positively damped resonance peak thanks to the wide control bandwidth of the UFCSs. The new harmonics resonance point at 1250 Hz can be triggered by the characteristic harmonics produced by the 12 pulse variable speed drive.

To illustrate the point, a 12 pulse variable speed drive harmonic current profile taken from field measurement(as shown in Fig. 8) was used. Ideal current source representing the harmonic profile of 10 such 12 pulse variable speed drives are connected via a 10/0.4 kV transformer to the MV grid (blue dashed line in Fig. 6).

Reading from the harmonic voltage distortion calculation results at MV bus 12 (Roelofs) in Fig. 9, it is clearly visible that the characteristic current emission from the 12 pulse variable speed drives got amplified in the case of massive

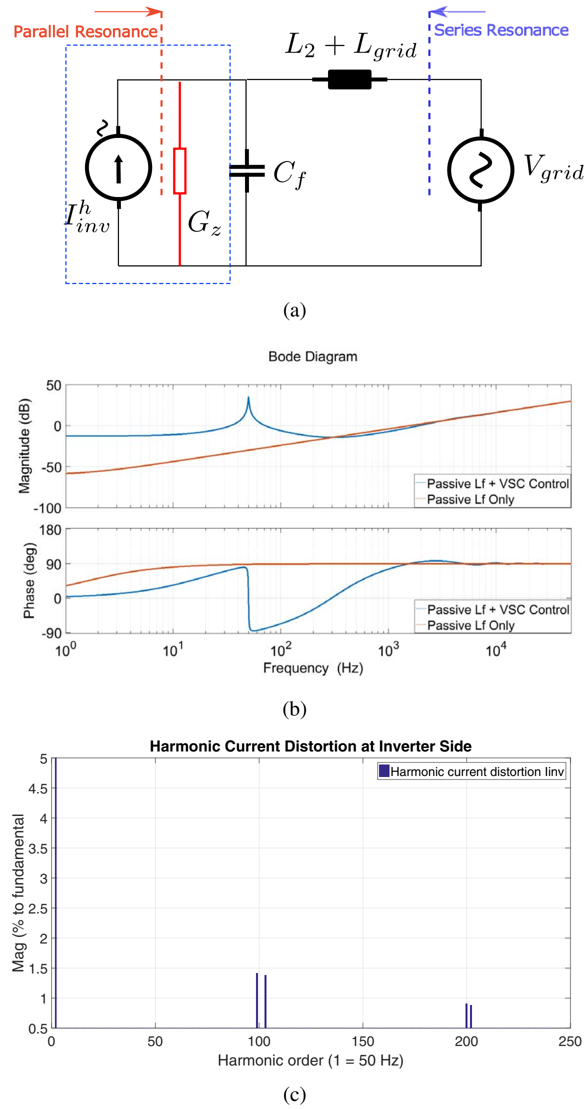

Fig. 5. Converer harmonic model for steady-state harmonic interaction study - (a) Norton equivalent circuit (b) Bode diagram comparision between pure passive inductor and passive inductor plus active inner control loop (c) Harmonic current emission from UFCS in percentage to the fundamental nominal current

UFCSs integration (blue bar in Fig. 9) in comparison to the base case value (red bar in Fig. 9). Henceforth, when it comes to future integration of UFCS, DNO shall carefully assess the new grid resonance point as a result of UFCS grid integration, and it is of high importance to shift the new grid resonance point away from the characteristic harmonic emissions (e.g. 5th, 7th, 11th ,13th, 23th, 25th etc).

V. Conclusions and Recommendations

This article discusses a harmonic resonance risk when a VSC based power converter, such as a UFCS, is introduced in a MV grid. The massive integration of UFCS in the future can possibility shift the original network frequency to the point that coincides with the characteristic harmonics emission from typical 12 pulse motor-drive as illustrated in the Dutch MV grid

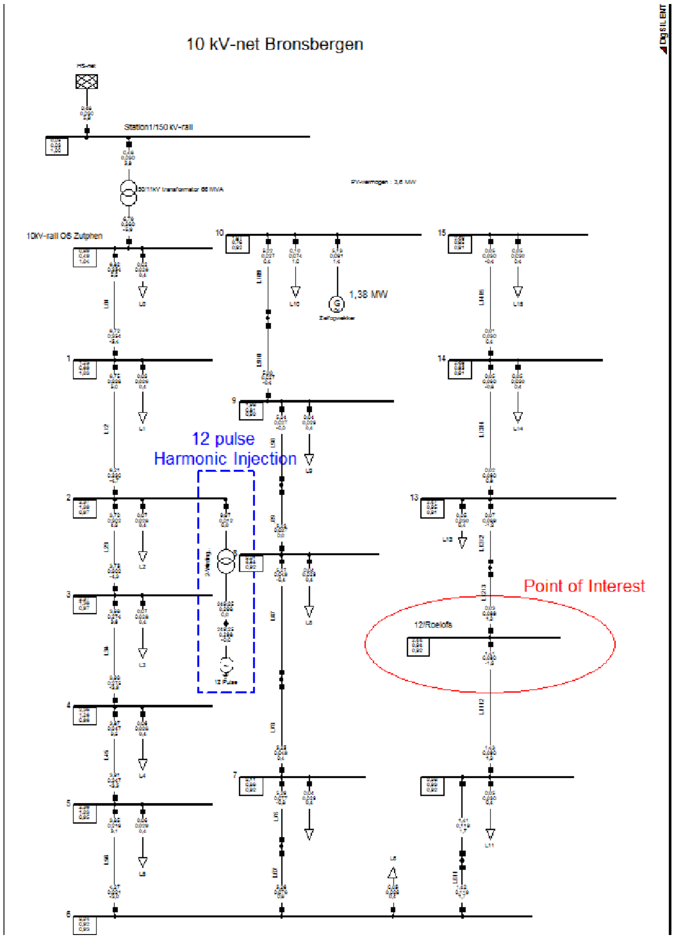

Fig. 6. Single line diagram of 10kV Bronsbergen MV network

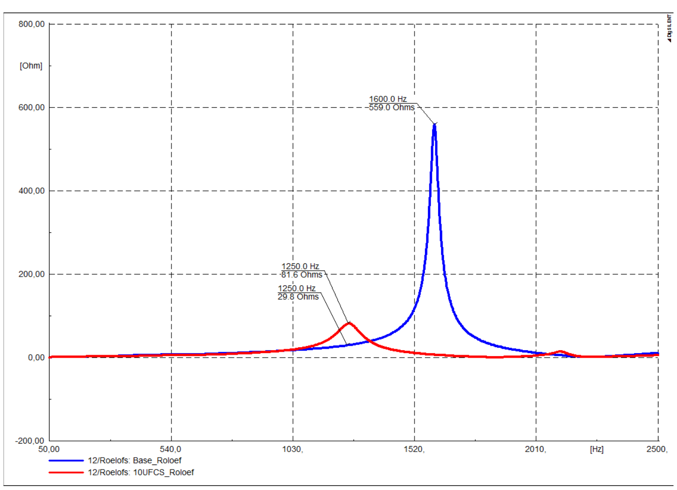

Fig. 7. Frequency sweep results at MV bus 12 (Roelofs) with and without UFCS connections

case study. The proposed converter harmonic model, compared to the ideal current source approach, delivers the required level of insight for the distribution network operators(DNOs). Future work will focus on benchmarking the harmonic distortion calculation results obtained from powerfactory based on the

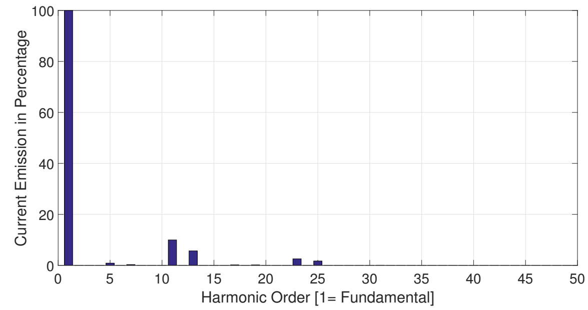

Fig. 8. 12 pulse variable speed motor drive harmonic current emission taken from measurement $I_{nom} = 250$ Amps

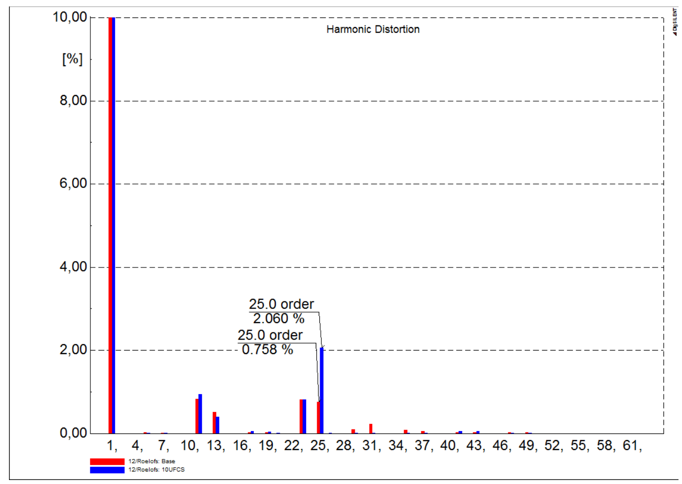

Fig. 9. Harmonic voltage distortion at MV bus 12 (Roelofs) with and without UFCS connections

converter harmonics model with the detailed PSCAD model on the same study case.

REFERENCES

[1] C. Corchero, M. Cruz-Zambrano, F. J. Heredia, J. I. Cairo, L. Igualada-Gonzalez, and A. Romero-Ortega, "Optimal sizing of microgrids: A fast charging station case," *9th International Conference on the European Energy Market, EEM 12*, pp. 1–6, 2012.

[2] H. N. Røstvik, "Norway's electric vehicle deployment success. A historical review including plans for fast charging stations covering all of the country - By 2015," *2013 World Electric Vehicle Symposium and Exhibition, EVS 2014*, vol. 1994, no. 2, pp. 1–10, 2014.

[3] X. Dong, Y. MU, H. Jia, J. Wu, and X. Yu, "Planning of Fast EV Charging Stations on a Round Freeway," *IEEE Transactions on Sustainable Energy*, vol. 3029, no. c, pp. 1–1, 2016.

[4] H. Zhang, S. Moura, Z. Hu, and Y. Song, "PEV Fast-Charging Station Siting and Sizing on Coupled Transportation and Power Networks," *IEEE Transactions on Smart Grid*, vol. 3053, no. c, pp. 1–1, 2016.

[5] N. Leeprechanon, P. Phonrattanasak, and M. K. Sharma, "Optimal planning of public fast charging station on residential power distribution system," *2016 IEEE Transportation Electrification Conference and Expo, Asia-Pacific (ITEC Asia-Pacific)*, no. June, pp. 519–524, 2016.

[6] M. Cruz-Zambrano, C. Corchero, L. Igualada-Gonzalez, and V. Bernardo, "Optimal location of fast charging stations in Barcelona: A flow-capturing approach," *International Conference on the European Energy Market, EEM*, 2013.

[7] N. Rastegarfar, B. Kashanizadeh, M. Vakilian, and S. A. Barband, "Optimal placement of fast charging station in a typical microgrid in Iran," *International Conference on the European Energy Market, EEM*, 2013.

[8] G. Celli, G. G. Soma, F. Pilo, F. Lacu, S. Mocci, and N. Natale, "Aggregated Electric Vehicles load profiles with Fast Charging Stations,"
[9] Y. H. Febriwijaya, A. Purwadi, A. Rizqiawan, and N. Heryana, "A study on the impacts of DC Fast Charging Stations on power distribution system," *Proceedings of 2014 International Conference on Electrical Engineering and Computer Science, ICEECS 2014*, no. November, pp. 136–140, 2014.
[10] C. Farkas, G. Szucs, and L. Prikler, "Grid impacts of twin EV fast charging stations placed alongside a motorway," *IYCE 2013 - 4th International Youth Conference on Energy*, pp. 1–6, 2013.
[11] K. Yunus, H. Zelaya De La Parra, and M. Reza, "Distribution grid impact of Plug-In Electric Vehicles charging at fast charging stations using stochastic charging model," *Proceedings of the 2011 14th European Conference on Power Electronics and Applications*, pp. 1–11, 2011.
[12] B. Pea-Da and S. Dechanupaprittha, "Impact of fast charging station to voltage profile in distribution system," *2014 International Electrical Engineering Congress, iEECON 2014*, pp. 3–6, 2014.
[13] G. Mauri, D. Bertini, E. Fasciolo, and S. Fratti, "22 nd International Conference on Electricity Distribution Paper 1266 THE IMPACT OF EV ' S FAST CHARGING STATIONS ON THE MV DISTRIBUTION GRIDS OF THE MILAN METROPOLITAN AREA 22 nd International Conference on Electricity Distribution," vol. 5, no. 1266, pp. 22–24, 2013.
[14] G. Celli, S. Mocci, F. Pilo, G. G. Soma, and E. Fasciolo, "Distribution Network Planning in Presence of Fast Charging Stations for Ev," *22nd International Conference on Electricity Distribution - CIRED*, no. 1500, pp. 1–4, 2013.
[15] C. H. Dharmakeerthi, N. Mithulananthan, and T. K. Saha, "Modeling and planning of EV fast charging station in power grid," *IEEE Power and Energy Society General Meeting*, pp. 1–8, 2012.
[16] R. Shi, X. P. Zhang, S. M. Ieee, D. C. Kong, N. Deng, and P. Y. Wang, "Dynamic impacts of fast-charging stations for electric vehicles on active distribution networks," *Innovative Smart Grid Technologies - Asia (ISGT Asia), 2012 IEEE*, pp. 1–6, 2012.
[17] A. Javadi, A. Ndtoungou, H. F. Blanchette, and K. Al-Haddad, "Power Quality Device for Future Household Systems with Fast Electric Vehicle Charging Station," *2015 IEEE Vehicle Power and Propulsion Conference, VPPC 2015 - Proceedings*, 2015.
[18] D. Aggeler, F. Canales, H. Zelaya - De La Parra, A. Coccia, N. Butcher, and O. Apeldoorn, "Ultra-fast DC-charge infrastructures for EV-mobility and future smart grids," *IEEE PES Innovative Smart Grid Technologies Conference Europe, ISGT Europe*, pp. 1–8, 2010.
[19] L. Tan, B. Wu, and S. Rivera, "A bipolar-DC-bus EV fast charging station with intrinsic DC-bus voltages equalization and minimized voltage ripples," *IECON 2015 - 41st Annual Conference of the IEEE Industrial Electronics Society*, pp. 2190–2195, 2016.
[20] M. Vasiladiotis, A. Rufer, and A. Béguin, "Modular converter architecture for medium voltage ultra fast EV charging stations: Global system considerations," *2012 IEEE International Electric Vehicle Conference, IEVC 2012*, pp. 1386–1393, 2012.
[21] G. Waltrich, J. L. Duarte, and M. A. M. Hendrix, "Power flow steering for electric vehicle fast charging station," *2012 IEEE Energy Conversion Congress and Exposition, ECCE 2012*, pp. 3062–3069, 2012.
[22] J. C. G. Justino, T. M. Parreiras, and B. J. C. Filho, "Hundreds kW Charging Stations for e-Buses Operating under Regular Ultra-Fast Charging," *IEEE Transactions on Industry Applications*, vol. 52, no. 2, pp. 1766–1774, 2016.
[23] B. Charger, "Ultra-Fast Charging Station for Electric Vehicles with integrated split Grid Storage Daniel Christen , Felix Jauch , J urgen Biela Laboratory for High Power Electronic Systems , ETH Zurich Email : christen@hpe.ee.ethz.ch URL : http://www.hpe.ee.ethz.ch/," *2015 17th European Conference on Power Electronics and Applications (EPE'15 ECCE-Europe)*, pp. 1–11, 2015.
[24] Z. Zhang, H. Xu, L. Shi, D. Li, and Y. Han, "A unit power factor DC fast charger for electric vehicle charging station," *Conference Proceedings - 2012 IEEE 7th International Power Electronics and Motion Control Conference - ECCE Asia, IPEMC 2012*, vol. 1, pp. 411–415, 2012.
[25] M. Ahmadi, N. Mithulananthan, and R. Sharma, "Dynamic load control at a bidirectional DC fast charging station for PEVs in weak AC grids," *Asia-Pacific Power and Energy Engineering Conference, APPEEC*, vol. 2016-Janua, pp. 4–8, 2016.
[26] J. Shi, Y. Liu, Y. Tang, and J. Deng, "Application of a hybrid energy storage system in the fast charging station of electric vehicles," *IET Generation, Transmission & Distribution*, vol. 10, no. 4, pp. 1092–1097, 2016.
[27] T. Dragičević, S. Bo, E. Schaltz, and J. M. Guerrero, "Flexible local load controller for fast electric vehicle charging station supplemented with flywheel energy storage system," *2014 IEEE International Electric Vehicle Conference, IEVC 2014*, 2015.
[28] G. Joos, M. De Freige, and M. Dubois, "Design and simulation of a fast charging station for PHEV/EV batteries," *EPEC 2010 - IEEE Electrical Power and Energy Conference: "Sustainable Energy for an Intelligent Grid"*, 2010.
[29] Ł. H. Kocewiak, C. Álvarez, and P. Muszynski, "Wind Turbine Harmonic Model and Its Application Overview , Status and Outline of the new IEC Technical Report," in *14th International Workshop on Large-Scale Integration of Wind Power into Power System as well as on Transmission Networks for Offshore Wind Power Plants*, (Brussels), 2015.
[30] F. Wang, J. L. Duarte, M. A. M. Hendrix, and P. F. Ribeiro, "Modeling and analysis of grid harmonic distortion impact of aggregated DG inverters," *IEEE Transactions on Power Electronics*, vol. 26, no. 3, pp. 786–797, 2011.
[31] X. Wang, F. Blaabjerg, and P. C. Loh, "An Impedance-Based Stability Analysis Method for Paralleled Voltage Source Converters," *The 2014 International Power Electronics Conference*, pp. 1529–1535, 2014.
[32] M. Cespedes and J. Sun, "Impedance modeling and analysis of grid-connected voltage-source converters," *IEEE Transactions on Power Electronics*, vol. 29, no. 3, pp. 1254–1261, 2014.
[33] X. Wang, L. Harnefors, and F. Blaabjerg, "A Unified Impedance Model of Grid-Connected Voltage-Source Converters," *IEEE Transactions on Power Electronics*, vol. PP, no. 99, pp. 1–1, 2017.
[34] D. Pan, X. Ruan, C. Bao, W. Li, and X. Wang, "Capacitor-current-feedback active damping with reduced computation delay for improving robustness of LCL-type grid-connected inverter," *IEEE Transactions on Power Electronics*, vol. 29, no. 7, pp. 3414–3427, 2014.